ORGANOMETALLICS

Article

pubs.acs.org/Organometallics

Isolation and Characterization of a Class II Mixed-Valence Chromium(I)/(II) Self-Activating Ethylene Trimerization Catalyst

Indira Thapa,[†] Sandro Gambarotta,*[,†] Ilia Korobkov,[‡] Muralee Murugesu,[†] and Peter Budzelaar*[,§]

[†]Department of Chemistry, University of Ottawa, Ottawa, Ontario, Canada

[‡]X-ray Core Facility, University of Ottawa, Ottawa, Ontario, Canada

[§]Department of Chemistry, University of Manitoba, Winnipeg, Manitoba, Canada

Supporting Information

ABSTRACT: Reduction of the tetranuclear $\{[(t\text{-Bu})NPPh_2]Cr[\mu\text{-}(t\text{-Bu})NPPh_2]_2Cr\}_2(\mu\text{-Cl})_2$ (**1**) with either KC_8 or vinyl Grignard afforded the dinuclear, mixed-valence $(Me_3P)Cr[\mu\text{-}(t\text{-Bu})NPPh_2]_3Cr$ (**2**) with the two metals possessing distinctively different coordination environments. According to the formulation of **2** as Cr(I)/Cr(II) mixed-valence species, **2** acts as a self-activating catalyst, producing under pressure of ethylene a mixture of 1-butene and 1-hexene. Activation with three different activators selectively produced three different products, namely, 1-butene with TEAL, 1-hexene with DMAO/TEAL, and LAO-free highly linear HMWPE with DMAO. Mixtures of 1-hexene and 1-butene were also obtained upon activation with vinyl Grignard. In this case it was possible to isolate, albeit in very low yield, an intriguing butadiene/butadiene-diyl cluster, $\{[(\eta^4\text{-butadiene})Cr(\mu,\eta^4\text{-butadienediyl})(\mu\text{-NP})Mg]_2(\mu\text{-Cl})_4Mg(THF)_2\}\{[(THF)_3Mg]_2(\mu\text{-Cl})_3\}_2$ (**3**), which is also a highly selective self-activating trimerization catalyst.

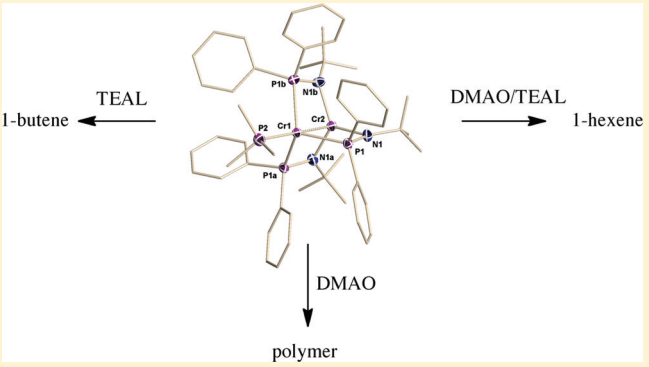

INTRODUCTION

Understanding the factors determining the selectivity of the ethylene oligomerization process[1] is central to designing catalysts with improved performance. Detailed mechanistic information may not only guide the fine-tuning of the reaction conditions but also enable switching of the catalytic behavior toward the most desired type of reactivity. In this quest, chromium complexes have proven to be particularly versatile since commercially viable catalysts have been discovered with this element for selective tri-[2] and tetramerization,[3] polymerization,[4] including highly linear UHMWPE,[5] and production of statistical distributions of oligomeric mixtures.[6] However, gaining a grasp on the factors that specifically direct the reactivity toward one of these transformations remains a challenge. On the other hand, an improved control would allow rational design of selective catalysts and of highly desirable switchable catalysts, i.e., species that may perform differently depending on the type of activation.

Recent work has linked the chromium oxidation state to the type of catalytic oligomerization.[7] Central to obtaining selective trimerization catalysts is the possibility of generating monovalent derivatives *in situ*. This is a nonstraightforward task in the sense that during the catalyst activation/reduction the divalent state must be bypassed[3d,8] to prevent formation of more stable divalent catalysts. In fact, these species often afford with high activity only statistical distributions of olefins[9] or polymers. In addition, the chromium redox dynamism may interconvert the three critical oxidation states (+III, +II, and +I) through disproportionations and comproportionations triggered by the aluminate activators. In turn, this decreases the selectivity of the catalytic cycle.[10] The ligand system obviously plays an important role in this respect since it may be able to stabilize a specific oxidation state by preventing or minimizing the occurrence of these reactions.

Our current studies are aimed at the preparation of reduced chromium species.[11] By endeavoring the isolation of such compounds we hope to obtain self-activating catalysts, which in turn could deepen our understanding of this fascinating catalytic process. The work by McGuinness,[1c,2j,12] Rosenthal,[13] Sasol Tech,[3a,14] Wass,[15] and ourselves[16] has clearly pointed out that the combination of nitrogen and phosphorus donor atoms in the same ligand framework may be a winning strategy to prepare selective oligomerization catalysts. We have observed that when an unsaturation is present in the ligand scaffold, the coordination of activators may occur, in turn causing self-activating as well as switchable behavior.[17] Among the large variety of ligand systems based on NP combinations we were interested in evaluating the behavior of the simplest congener, i.e., the readily prepared $(t\text{-Bu})N(H)PPh_2$ ligand. To our surprise, this simple system supports a great variety of polymetallic structures[18] that could in principle have potential vis-à-vis Rosenthal's polymetallic activation hypothesis.[19]

In this paper we describe the reduction of the tetranuclear and divalent $\{[(t\text{-Bu})NPPh_2]Cr[\mu\text{-}(t\text{-Bu})NPPh_2]_2Cr\}_2(\mu\text{-Cl})_2$ (**1**)[18] to an unusual mixed-valence, self-activating catalyst.

Received: November 25, 2011

   dx.doi.org/10.1021/om201181n | *Organometallics* XXXX, XXX, XXX–XXX

RESULTS AND DISCUSSION

The reduction of **1** was easily achieved by stirring its THF solutions with freshly prepared KC_8 and in the presence of a small excess of PMe_3. The reaction afforded the new mixed-valence species $(Me_3P)Cr[\mu\text{-}(t\text{-}Bu)NPPh_2]_3Cr$ (**2**) in crystalline form (Scheme 1).

Scheme 1

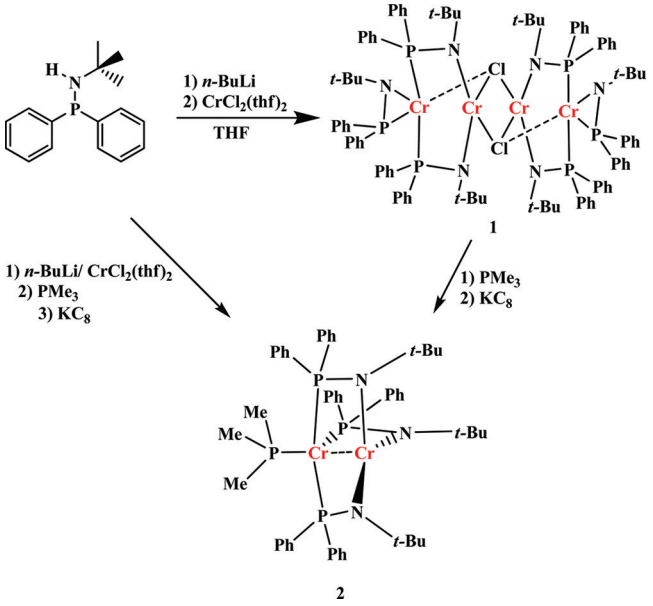

The connectivity of **2** was revealed by an X-ray crystal structure (Figure 1) showing a dinuclear core with the two

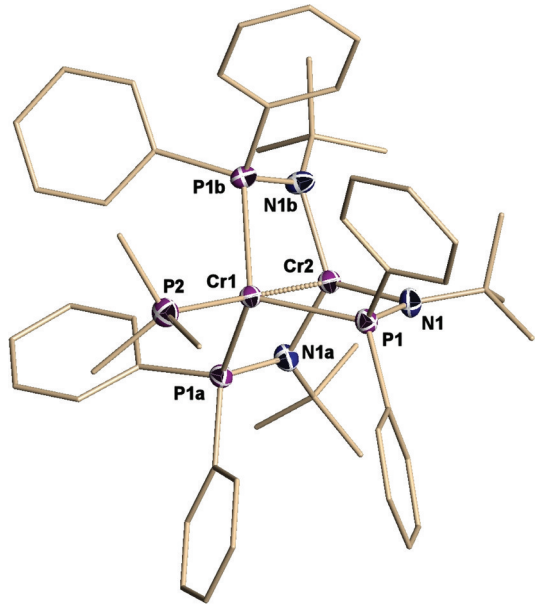

Figure 1. Partial thermal ellipsoid drawing of complex **2** (50% probability level).

metal centers bridged by three *t*-BuNPPh$_2$ anions. The ligands are identically placed with respect to the dimetallic unit in the sense that one metal is exclusively bonded to the P atoms and the second only to the nitrogens. The chromium bonded to the phosphorus atoms [Cr(1)−P(1) = 2.4431(4) Å, P(1)−Cr(1)−P(2) = 108.569(13)°] is also coordinated to the P atom of a Me_3P unit [Cr(1)−P(2) = 2.5008(8) Å] in an overall tetrahedral environment [P(1)−Cr(1)−P(1a) = 110.356(13)°, P(1)−Cr(1)−P(1b) = 110.359(13)°, P(1a)−Cr(1)−P(1b) = 110.357(13)°].

The three nitrogen atoms of the three ligand amino residues chelate the second chromium atom [Cr(2)−N(1) = 2.0172(13) Å] and provide a trigonal-planar coordination geometry [N(1)−Cr(2)−N(1a) = 119.814(6)°]. The Cr−Cr distance [Cr(1)···Cr(2) = 2.3124(6) Å] is short and falls in what is normally regarded as a Cr−Cr multiple bonding range.

The charge count of complex **2** suggests two different interpretations of the structure that can be regarded as either a Cr(III)/Cr(0) or a Cr(II)/Cr(I) mixed-valence species. The two distinctively different coordination environments indicate that in any scenario the complex may be regarded as a class II mixed-valence species. The trigonal-planar environment of the chromium atom surrounded by the three nitrogens is strongly reminiscent of that of a few existing Cr(III) amido complexes.[20] In turn this will require the second chromium atom to be zerovalent. However, the close proximity at Cr−Cr bonding distance makes such a large charge unbalance between the two metals unlikely. Therefore, a Cr(II)/Cr(I) formulation is perhaps more realistic.

Magnetic properties measured at variable temperature were not particularly informative in this respect (Figure 2), showing only a Curie−Weiss type of behavior (C = 0.4 and θ = −2.8 K) with the value of the magnetic moment leveling at room temperature over the 1.7 μ_{BM} as expected for a S = 1/2 species. Also the behavior of the magnetization against the field did not reveal unexpected features (see Supporting Information (SI), Figure S-1) other than the presence of less than 5% of paramagnetic impurities. These impurities are most likely inherent to the sample preparation technique of a material of such enhanced air sensitivity.

Unrestricted DFT calculations were undertaken to elucidate the electronic structure and the oxidation states of the two metals in **2**. Results for the simplified models $Cr^{II}(\mu\text{-}MeNPMe_2)_3Cr^{I}(PMe_3)$ and $Cr^{II}(\mu\text{-}^{t}BuNPMe_2)_3Cr^{I}(PMe_3)$ gave very similar results, and only the former one (which gives cleaner MO pictures) will be discussed here. The three NP ligands are best considered as bearing a charge of −1 each. That results in a *total* oxidation state of +III divided over the two Cr atoms. The experimentally observed doublet ground state would be compatible with either two low-spin Cr centers or antiferromagnetic coupling between two high-spin Cr centers. In view of the low coordination numbers of both chromium atoms, the latter interpretation seems more reasonable. According to the calculations, the electronic structure is best interpreted as having the N-bound Cr in the +II oxidation state, while the P-bound Cr is assigned an oxidation state of +I. The pattern of occupied orbitals (see Table 1) is entirely consistent with an interpretation of antiferromagnetic coupling between a high-spin Cr(I) and a high-spin Cr(II) center. For such antiferromagnetic coupling, this type of spin-unrestricted calculation necessarily produces solutions that are impure spin states, but the picture arising from the calculation seems reasonable.

The Cr(I) center has a high-spin configuration with each 3d orbital singly occupied.[21] This would therefore be consistent with a highly symmetric metal environment. The Cr(II) metal center, however, has an empty $d_{x^2-y^2}$ orbital. Since this is one of the *pair* (d_{xy}, $d_{x^2-y^2}$) of the correct shape to overlap with the N lone pair orbitals, one would expect a Jahn−Teller distortion,

dx.doi.org/10.1021/om201181n | *Organometallics* XXXX, XXX, XXX−XXX

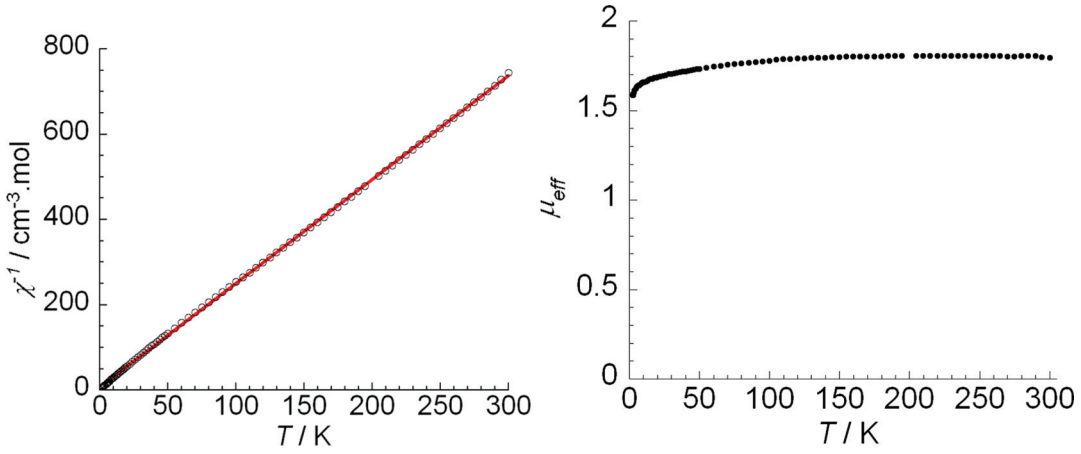

Figure 2. Diagrams of the inverse of the magnetic susceptibility (left) and of the magnetic moment (right) versus temperature. Solid line represents the fit obtained using Curie–Weiss law.

Table 1. Occupied α and β Orbitals for $Cr^2(\mu\text{-}MeNPMe_2)_3Cr^1(PMe_3)$[a]

α (HOMO = 119)		β (HOMO = 118)	
119	Cr^1 d_{xz}	118	Cr^1 d_{xz}
118	Cr^2 d_{xy}	117[b]	Cr^1 d_{z2}+...
117	Cr^2 d_{Z2}+...	116	Cr^1 d_{yz}-NP
115	Cr^2 d_{xz}	115	Cr^1 d_{yz}+NP
114	Cr^2 d_{yz}	114[b]	Cr^1 d_{x2-y2}

[a] α116 is a combination of N p_π orbitals. For orbital labeling, the z-axis was chosen along the Cr–Cr vector; x and y labels are arbitrary. Orientations are different for the different orbitals to better illustrate their shapes. [b] Orientations of β117 and β114 are not nicely aligned with coordinate axes.

and indeed the optimized structure is not perfectly symmetric. However, the deviations from perfect C_{3v} symmetry are modest even for the model complexes. It seems reasonable to assume that for the highly sterically hindered real systems steric factors will maximize the distances between the NP ligands and hence favor an even more symmetric structure, thus explaining the observed 3-fold symmetry.

The occupied orbitals show very little evidence of metal–metal bonding. In both α117 and β117 (occupied Cr d_{z^2} orbitals) there is only a small contribution from the second Cr center (contributing to the Cr–Cr σ-bond). The other orbitals show even less evidence for metal–metal π- and/or δ-bonding. Thus, this complex seems to be another example of a Cr dimer where the short Cr–Cr distance is enforced or promoted by the ligand skeleton (with no "objection" by the Cr atoms) rather than by a strong metal–metal bond.[22] Accordingly, one could envisage that ligand rearrangement/redistribution could easily lead to fragmentation of the dimer into two monometallic fragments.

Complex **2** shows an interesting catalytic behavior for ethylene oligo- and polymerization (Table 2). As expected for a reduced species capable of feeding the catalytic cycle with low-valent chromium, the complex is also self-activating. Under pressure of ethylene gas, the complex produces a mixture of 1-butene and 1-hexene and no polymer. As commonly observed for self-activating catalysts, the activity was low, likely due to both the difficulties to eliminate impurities from the reaction mixture and also the fact that only one of the two metal centers may produce catalytic behavior under the self-activating conditions. Assuming that the catalytically self-activating species is the unit containing the monovalent center, the formation of 1-hexene as a major component has to be expected. Instead the formation of the relatively large amount of 1-butene could be generated through a different path. In fact, in the ring expansion mechanism, reductive elimination is not expected to occur at the level of the five-membered ring.[21] The fact that the reaction is sensitive to the nature of the solvent fits instead with the poisoning effect of toluene on monovalent chromium catalysts.[10]

Activation with MAO produced only small amounts of PE. However an interesting catalytic activity was observed upon activation with TMA-depleted MAO (DMAO). The polymer formed with this activator was nearly perfectly linear with reasonable polydispersity and a very high molecular weight (M_w = 980 423, PDI = 2.7). In addition, the high-T ^{13}C NMR spectrum showed the polymer being highly linear. To assess the role of TMA present in MAO, we have also tested **2** with pure TMA. The reaction in this case produced no polymer and only a comparable amount of 1-butene and 1-hexene with low

dx.doi.org/10.1021/om201181n | Organometallics XXXX, XXX, XXX–XXX

Table 2. Catalytic Testing[a]

cat., solv.	co-cat. (equiv)	activity (g/mmol/cat./h)	PE (g)	oligom. (g)	C_4 (%)	C_6 (%)	C_8 (%)	$>C_{10}$ (%)
2, toluene		60		1.5	30	70		
2, MeCy		120		3.0	30	65	5	
2, toluene	MAO (500)	160	4	traces				
2, MeCy	MAO (150)	340	8	traces				
2, MeCy	DMAO (400)	1504	38					
2, MeCy	TMA(10)	40		1.0	52	48		
2, MeCy	DMAO(400)/TEAL (20)	200		5		95	5	
2, MeCy	TEAL (20)	120	traces	3	99	traces		
2, MeCy	C_2H_3MgCl (2)	240		6	53	45	2	
3, MeCy[b]		280		7.5	traces	99		

[a]Conditions: 50 μmol catalyst loading, 40 bar of ethylene, 30 min reaction time, total volume 100 mL at 100 °C. [b]5 μmol catalyst loading.

activity. By adding to DMAO a small amount of the more reducing TEAL, highly pure 1-hexene free of 1-butene and polymer was obtained, the only contaminant being a small amount of 1-octene. Remarkably, activation by TEAL alone resulted in the exclusive formation of 1-butene.

The self-activating behavior of **2** is intriguing, and it can be rationalized with the ability of **2** to feed monovalent species directly into the catalytic cycle. The switchable behavior observed as a function of the nature of the activator is instead hard to comprehend. It indicates that the aluminates may clearly trigger formation of two different catalytically active species, namely, full reduction (as in the case of DMAO/TEAL) or disproportionative oxidation (as in the case of DMAO).

In search for clues, possible trimerization and dimerization cycles, briefly highlighted in Scheme 2, were computationally

Scheme 2

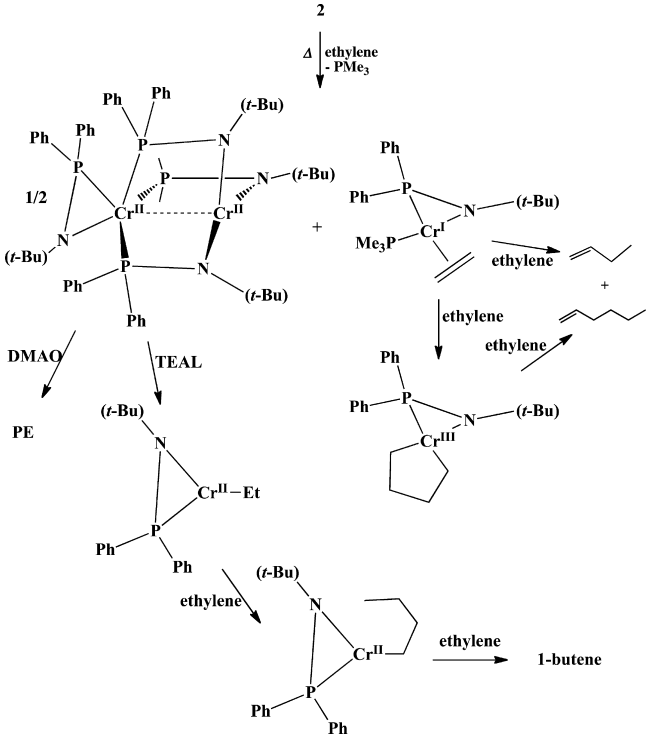

investigated. For the trimerization cycle we have examined the minimal [Me_2PNMe]Cr catalytic center, assuming that [Ph_2PN*t*-Bu]Cr fragments may be generated by the dissociation of **2** in the presence of ethylene. Spin states S = 1/2, 3/2, and 5/2 were considered. The S = 3/2 spin state was found to be lowest in energy for all stages of the reaction except the mono-olefin complexes, where S = 5/2 was preferred. S = 1/2 states were systematically about 20 kcal/mol higher in energy than S = 3/2 states. The reaction profile is summarized in Figure 3, and energies are collected in Table 3.

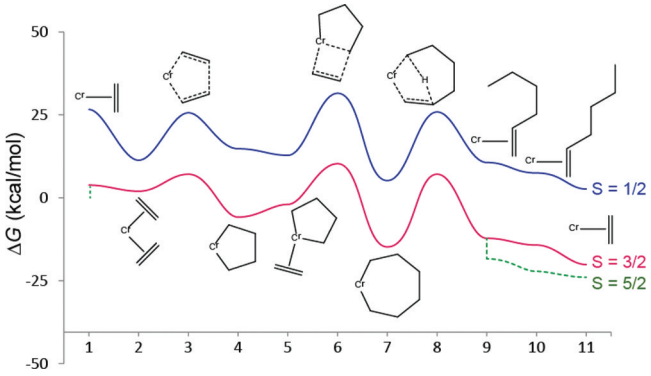

Figure 3. Free energy profile (kcal/mol) for 1-hexene formation at a [Me_2PNMe]Cr center. The S = 5/2 state is only relevant for Cr(I) mono-olefin complexes. The final Cr(C_2H_4) complex is shown lower than the initial one because on going from 1 to 11, one molecule of 1-hexene has been produced.

Table 3. Calculated Relative Free Energies (kcal/mol) for Catalytic 1-Hexene Formation

stage[a]	S = 1/2	S = 3/2	S = 5/2
1	26.61	3.85	0.00
2	11.30	2.01	
3	25.64	7.14	
4	14.79	−5.83	
5	12.79	−2.00	
6	31.51	10.28	
7	5.22	−14.80	
8	25.89	7.12	
9	10.65	−12.18	−18.37
10	6.81	−14.25	−22.19
11	2.64	−20.12	−23.97

[a]For structures, see Figure 3.

The initially formed [Me_2PNMe]Cr(C_2H_4) prefers the S = 5/2 spin state. However, in this state the system does not bind a second ethene molecule. After a switch to S = 3/2, a second ethene molecule does bind, at a free energy close to the starting S = 5/2 monoethene complex. [Me_2PNMe]Cr(C_2H_4)$_2$ undergoes

dx.doi.org/10.1021/om201181n | Organometallics XXXX, XXX, XXX–XXX

very easy C−C coupling to the corresponding metallacyclopentane complex, with a barrier of only about 5 kcal/mol. Binding an additional ethene molecule is now endergonic by just 4 kcal/mol, and its insertion has a barrier of 12 kcal/mol. The subsequent $\beta \rightarrow \omega$ hydrogen transfer is the most difficult step of the reaction, with a calculated free energy barrier of 22 kcal/mol. After that, a spin flip back to $S = 5/2$ occurs, and the final step is exchange of ethene for hexene. Geometries of the various stages of the reactions are given as SI (Figure S1).

Ligand hemilability seems to be a common theme for trimerization catalysts. Indeed, the PN model ligand used here also displays rather variable Cr−P distances, which *are not dictated by steric effects*. Interestingly, there is also no obvious link with electronic unsaturation. Thus, we see relatively short Cr−P distances for the bis(ethene) complex, the metallacyclopentane, its ethene complex, the insertion TS, and the resulting metallacyclohexane, but longer Cr−P distances for the ethene coupling TS and the H transfer TS. Inspection of preferred relative orientations of amide and hydrocarbon fragments suggests that the amide nitrogen also functions as a π-donor, so the complexes studied are less electronically unsaturated than one might expect for such low coordination numbers.

In addition to trimerization, we have also studied a simple model for the selective ethene dimerization observed upon activation (following the traditional insertion mechanism). Given that elimination of 1-butene from the five-membered metallacycle is energetically less favored (but not impossible),[21] we have considered the possibility that the divalent partner of the initial dissociation of **2** might be responsible for it. Upon activation with TEAL, such a species might be transformed into [Me_2PNMe][Me_3P]Cr(Et) (a species such as [Me_2PNMe]Cr(Et) was considered to be too unsaturated to be realistic). As long as the PN ligand remains N-monodentate, one would expect standard square-planar Cr(II) insertion chemistry for [Me_2PNMe][Me_3P]Cr(Et) upon coordination of ethylene, and we assumed an $S = 2$ spin state throughout the cycle. Indeed, we see this coordination mode for most of the cycle (Figure 4,

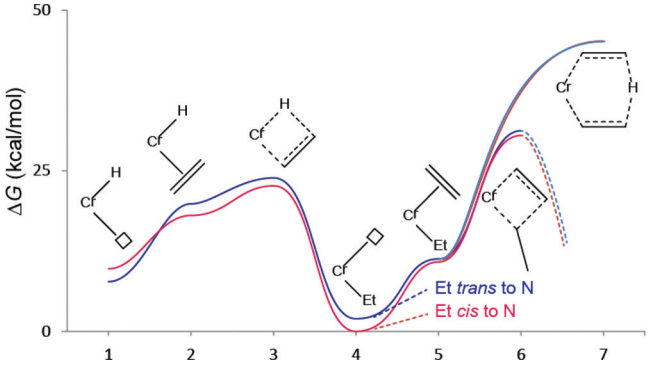

Figure 4. Free energy profile for 1-butene formation at [Me_2PNMe][Me_3P]Cr(Et) ($S = 2$).

Table 4, Figure S-3). Only the coordinatively unsaturated CrEt and CrH species preferentially adopt geometries in which the PN ligand becomes η^2-bound, thus relieving the electronic unsaturation. In addition, for some olefin complexes we located geometries that are closer to five-coordinate, with the H or Et in a *fac* orientation relative to N and the phosphine ligand.

Table 4. Calculated Relative Free Energies (kcal/mol) for 1-Butene Formation at [Me_2PNMe][Me_3P]Cr(Et)

	Et *trans* to N	Et *cis* to N
1	7.76	9.74
2	19.87	18.06
3	23.90	22.67
4	1.97	0.00
5	11.30	10.80
6	31.25	30.49
7	45.31	45.31

[a]For structures, see Figure 4.

These do not appear to play a prominent role in the insertion chemistry.

Therefore, 1-butene formation in this system appears to follow the standard insertion/elimination mechanism, although insertion barriers are rather high, perhaps reflecting the low electrophilicity of the metal center. The β-elimination from the ethyl complex to give the hydride-ethene complex and even subsequent loss of ethene are easier than insertion. Interestingly, concerted β-H transfer to monomer is very difficult for this system. The transition state for this step does not involve any close Cr−H interaction but rather resembles the "alternative" transfer TS geometry studied systematically by Talarico and Budzelaar.[22]

We have also tried to model alternative chain growth mechanisms involving Cr(I), as well as possible trimerization cycles involving Cr(II)/Cr(IV) or Cr(0)/Cr(II), but none of these variations produced a viable cycle. Therefore, we believe the above results at least suggest that a Cr(I)/Cr(III) cycle is reasonable for 1-hexene and, to a minor extent, 1-butene formation, while insertion chemistry is more consistent with a Cr(II) species. One new idea derived from the above data is that for these species of low electrophilicity β-H elimination rather than β-H transfer may be responsible for low molecular weight polymers, oligomers, or S−F distributions.

We have also attempted the activation of **2** with vinyl Grignard. This was advised by recent results from our lab showing that the oxidative coupling of two vinyl anions bonded to chromium may trigger two-electron reduction to the monovalent state, thus producing self-activating selective trimerization catalysts.[11] Upon treatment of **2** with two equivalents of vinyl Grignard and exposure to ethylene, the catalytic system displayed a behavior very comparable to that observed with TMA, affording the same mixture of 1-butene and 1-hexene, just with higher activity. We further observed that during the activation process of **2** with vinyl Grignard the color changed from reddish-brown to brown. Occasionally, a few crystals of a new compound were formed with very low yield. Regrettably, attempts to improve the reaction yield to enable complete characterization failed, and even the reproducibility of the crystal formation was random. Nonetheless, the quality of the crystals was always sufficient for crystal structure determination, allowing to formulate this new species as {[(η^4-butadiene)Cr(μ-η^4:η^1-butadien-diyl)(μ-NP)Mg]$_2$(μ-Cl)$_4$Mg(THF)$_2$}{[(THF)$_3$Mg]$_2$(μ-Cl)$_3$}$_2$ (**3**).

Complex **3** is a symmetry-generated dimer (Figure 5) where each of the two identical (η^4-butadiene)Cr(μ-η^4:η^1-butadienediyl)(μ-NP)Mg units is connected to a central magnesium cation via two bridging chlorine atoms. Two unconnected {[(THF)$_3$Mg]$_2$(μ-Cl)$_3$} cations per dimeric unit complete the structure. The chromium-containing unit shows the chromium

dx.doi.org/10.1021/om201181n | *Organometallics* XXXX, XXX, XXX−XXX

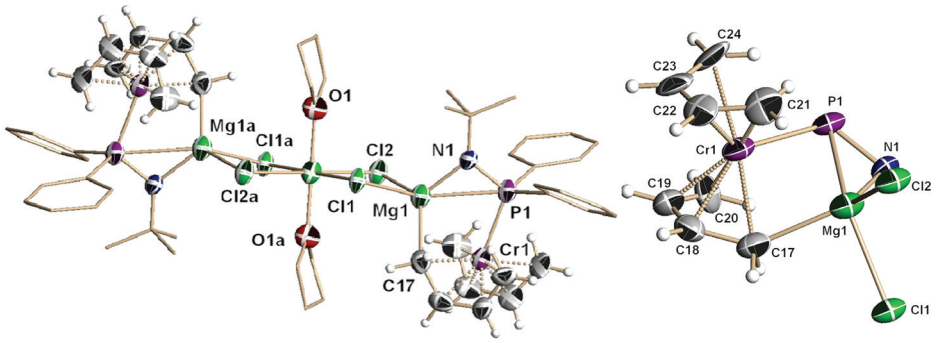

Figure 5. (Left) Partial thermal ellipsoid drawing of the dianionic moiety of complex **3** (50% probability level). (Right) simplified view of the chromium-containing unit. The two $\{[(THF)_3Mg]_2(\mu\text{-}Cl)_3\}$ cations have been omitted for clarity.

Scheme 3

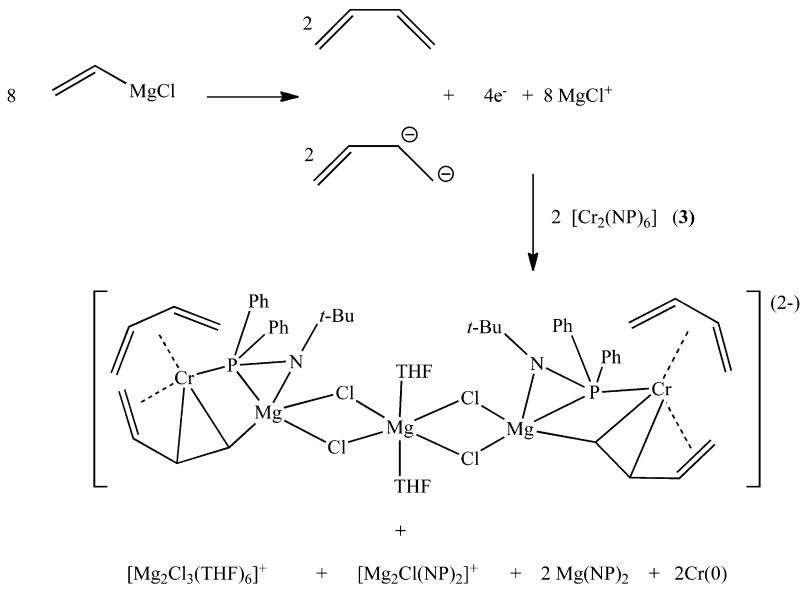

atom sandwiched between two π-bonded butadiene units. The first butadiene residue displays the expected bond distances [C(21)−C(22) = 1.406(9) Å; C(22)−C(23) = 1.432(10) Å; C(23)−C(24) = 1.400(9) Å; Cr(1)−C(21) = 2.204(7) Å; Cr(1)−C(22) = 2.095(7) Å; Cr(1)−C(23) = 2.083(7) Å; Cr(1)−C(24) = 2.179(7) Å] and angles [C(22)−Cr(1)−C(21) = 38.1(2)°; C(23)−Cr(1)−C(22) = 40.1(3)°; C(23)−Cr(1)−C(24) = 38.3(2)°; C(22)−Cr(1)−C(24) = 70.0(3)°; C(23)−Cr(1)−C(21) = 69.6(3)°; C(24)−Cr(1)−C(21) = 79.9(3)°], comparing well with those of other Cr butadiene derivatives. The second instead appears to be unusual in the sense that one C−C bond with the terminal C σ-bonded to a Mg cation displays a distance indicative of a C−C single bond [C(17)−C(18) = 1.471(8) Å]. The other two carbon−carbon distances in the same ligand are closer to what would be expected for C−C double bonds [C(18)−C(19) = 1.400(9) Å; C(19)−C(20) = 1.384(8) Å]. In addition, the Cr−C distances to the internal two C atoms of this ligand are relatively short [Cr(1)−C(18) = 2.105(7) Å; Cr(1)−C(19) = 2.088(7) Å]. The NP ligand bridges chromium to magnesium [N(1)−Mg(1)−Cr(1) = 87.06(17)°; P(1)−Mg(1)−Cr(1) = 50.99(6)°]. However, only the P atom is bonded to chromium, while both donor atoms are in the bonding range with magnesium [Cr(1)−P(1) = 2.398(2) Å; Mg(1)−N(1) = 2.002(6) Å; Mg(1)−P(1) = 2.733(3) Å]. Two unconnected $[Mg_2Cl_3(THF)_6]^+$ countercations complete the structure.

The hydrogen atom positions of the two C_4 units were found by difference Fourier maps and satisfactorily refined with a minor decrease of the convergence factors and thus lending some credibility to their positions. Optimized structures of simplified, monochromium models (η^4-butadiene)Cr(μ,η^4-butadienediyl)-(μ-Me_2PNMe)Mg$(THF)_2$ and (η^4-butadiene)Cr(μ,η^4-butadien-diyl)(μ-Me_2PNMe)$MgCl_2^{2-}$ reproduced the observed structural features well and also support the above-mentioned H atom locations (see Figure S-5 in the SI).

The formation of **3** from **2** has no simple explanation (Scheme 3). We have recently described the utilization of vinyl Grignard for the formation of monovalent chromium butadiene complexes[11] and butadiene-diyl derivatives. In the present case, each chromium atom in the dimetallic dianion of **3** bears both units. The difference with the previously reported butadiene-diyl compound is that the two formal negative charges appear to be located on two contiguous C atoms rather than on the two terminal ones.[11b] The coordination of Mg at the terminal carbon atom is probably responsible for this oddity. In any event, the vinyl coupling generates the electrons necessary for the reduction of the four chromium atoms to the two formally monovalent centers present in **3** and to metallic chromium that unavoidably was observed during the reactions of **2** with

dx.doi.org/10.1021/om201181n | *Organometallics* XXXX, XXX, XXX−XXX

activators. Due to the lower-than-stoichiometric amount of chlorine, the reaction stoichiometry can be balanced only by assuming that the magnesium countercations may redistribute in the reaction mixture among several species, with only that containing fully chlorinated $[Mg_2Cl_3(THF)_6]^+$ cations being able to crystallize into **3**. Incidentally, this could well explain the very low yield and difficulty in reproducing the crystallization. Nonetheless, the structure is of interest given the unprecedented arrangement around the chromium center. Also in agreement with the presence of the formal monovalent state, the complex is a self-activating catalyst exclusively producing 1-hexene under the usual reaction conditions. Different from the activation of **2** with vinyl Grignard, no 1-butene has been detected even in traces during the self-activation of **3**, consistent with the complex containing only Cr(I).

In conclusion, we have herein reported the isolation and full characterization of a Cr(I)/Cr(II) mixed-valence derivative of the anionic NP ligand. As expected for a reduced species, this complex is a self-activating catalyst. DFT calculations supported the idea that the monovalent species generates 1-hexene and 1-butene to a lesser extent, while the divalent unit is likely to be responsible for 1-butene through a different mechanism. The ability of activators to switch the behavior from polymerization to selective tri- or dimerization is the result of their ability to trigger the chromium redox dynamism.[10]

EXPERIMENTAL SECTION

All reactions were carried out under a dry nitrogen atmosphere. Solvents were dried using an aluminum oxide solvent purification system. The liquid product mixtures were analyzed by using a CP 9000 gas chromatograph (GC) equipped with a 30 mL × 0.32 mm i.d., capillary CP-Volamine column and a FID detector. All single-point experiments were performed in duplicate. The yield was determined by ^{1}H NMR spectroscopy (Varian Mercury 400 MHz spectrometer). Samples for variable-temperature magnetic susceptibility measurement were preweighed inside a drybox equipped with an analytical balance and measured using a Quantum Design SQUID MPMS-XL7 magnetometer operating between 1.8 and 300 K for dc-applied fields ranging from −7 to 7 T. Elemental analysis was carried out with a Perkin-Elmer 2400 CHN analyzer. Data for X-ray crystal structure determination were obtained with a Bruker diffractometer equipped with a 1K Smart CCD area detector. Vinyl Grignard (Aldrich), MAO (10 wt %, Aldrich), Me_3Al, and $Al(Et)_3$ (Strem) were used a received. DMAO was prepared by pumping *in vacuo* a solution of MAO for three days under moderate heating. NMR solutions were checked for the eventual and residual presence of TMA. Chromium salts were prepared according to standard procedures. The NP ligand was prepared according to published procedures. Complex **1** was prepared as described in a previous publication.[18]

Preparation of $(Me_3P)Cr[\mu$-(*t*-Bu)NPPh$_2]_3$Cr (2). *Method A.* A solution of *t*-BuN(H)P(Ph)$_2$ (0.25 g, 1.0 mmol) in THF (5 mL) was treated with a solution of *n*-BuLi in hexane (0.41 mL, 1.02 mmol, 2.5 M) at −10 °C. The reaction mixture was stirred overnight at room temperature and then combined with a suspension of $CrCl_2(THF)_2$ (0.27 g, 1 mmol) in THF (5 mL). Stirring was continued for 18 h. Neat trimethylphosphine (0.10 mL, 1 mmol) was added to the reaction mixture under continued stirring at room temperature. After 30 min, the color of the solution turned brown. Freshly prepared potassium graphite (0.27 g, 2.0 mmol) was added, and stirring continued at room temperature for a further 48 h. The solvent was evaporated *in vacuo*, and the solid residue was redissolved in diethyl ether. A small amount of insoluble gray material was separated by centrifugation, and the resulting brown solution was allowed to stand for 5 days at −35 °C. Brown paramagnetic crystals of **2** were filtered, washed with cold hexane, and dried *in vacuo* (0.02 g, 0.02 mmol, 20%). Anal. Calcd (Found) for $C_{51}H_{66}Cr_2N_3P_4$: C 64.55 (64.35), H 7.01 (6.88), N 4.43 (4.23). IR (cm^{-1}, Nujol mull): 2923b, 2854b (Nujol), 1975s, 1892m, 1819s, 1766m, 1580m, 1466m, 1430s, 1383s, 1358s, 1354s, 1203m, 1178s, 1085m, 1049 m, 1025s, 950s, 819m, 747s, 725s, 697s [μ_{eff} = 1.875 μ_B].

Method B. A green solution of **1** (0.23 g, 0.11 mmol) in THF (5 mL) was treated with neat trimethylphosphine (0.012 mL, 0.11 mmol) and stirred at room temperature for 30 min. Freshly prepared potassium graphite (0.03 g, 0.23 mmol) was added to the solution, and the resulting mixture was stirred at room temperature for a further 48 h. The solvent was evaporated *in vacuo*, and the solid residue was redissolved in diethyl ether. A small amount of insoluble gray material was separated by centrifugation, and the resulting brown solution was allowed to stand for 5 days at −35 °C. Brown paramagnetic crystals of **2** were filtered, washed with cold hexane, and dried *in vacuo* (0.09 g, 0.09 mmol, 85%).

Method C. A solution of *t*-BuN(H)P(Ph)$_2$ (0.25 g, 1 mmol) in THF (5 mL) was treated with a solution of *n*-BuLi in hexane (0.41 mL, 1.02 mmol, 2.5 M) at −10 °C. The reaction mixture was stirred overnight at room temperature and then combined with a suspension of $CrCl_2(THF)_2$ (0.27 g, 1 mmol) in THF (5 mL). Stirring was continued for 18 h. Neat trimethylphosphine (0.10 mL, 1 mmol) was added to the reaction mixture, and stirring was continued at room temperature for a further 30 min. By this time, the green color of the solution changed to brown. A solution of vinyl magnesium chloride (1.25 mL, 2 mmol, 1.6 M in THF) was added, and stirring was continued at room temperature for a further 18 h. Anhydrous dioxane (0.26 mL, 3 mmol) was then added. The solid formed during 12 h was removed by centrifugation. The solvent was evaporated *in vacuo*, and the solid residue was redissolved in diethyl ether. A small amount of colorless insoluble material was further eliminated by centrifugation, and the resulting brown solution was allowed to stand for 5 days at −35 °C. Brown paramagnetic crystals of **2** were filtered, washed with cold hexane, and dried *in vacuo* (0.20 g, 0.21 mmol, 21%).

Method D. A green solution of **1** (0.23 g, 0.11 mmol) in THF (5 mL) was added with neat trimethylphosphine (0.12 mL, 0.11 mmol). After 30 min, the mixture was added with vinylmagnesium chloride (0.14 mL, 0.23 mmol, 1.6 M in THF) and stirred at room temperature for 18 h. Dry dioxane (0.03 mL, 0.34 mmol) was added. After centrifugation, the solvent was evaporated *in vacuo* and the solid residue redissolved in diethyl ether. A small amount of colorless insoluble material was separated by centrifugation, and the resulting brown solution was allowed to stand for 5 days at −35 °C. Brown paramagnetic crystals of **2** were filtered, washed with cold hexane, and dried *in vacuo* (0.10 g, 0.10 mmol, 92%).

Isolation of {[(η^4-Butadiene)Cr(μ,η^4-butadienediyl)(μ-NP)-Mg]$_2$(μ-Cl)$_4$Mg(THF)$_2$}{[(THF)$_3$Mg]$_2$(μ-Cl)$_3$}$_2$(THF)$_{2.5}$ (3). A solution of **2** (0.12 g, 0.2 mmol, 1.6 M) in THF (10 mL) was treated with vinylmagnesium chloride (2.5 mL, 1.6 M in THF) at room temperature. The reaction mixture was stirred for 2 h at room temperature. The color changed to dark brown, and dioxane was added (0.026 g, 0.3 mmol). A small amount of insoluble material was separated by centrifugation, and the resulting brown solution was allowed to stand for two days at −35 °C. A few orange-colored paramagnetic crystals of **1** were obtained, which were washed with cold hexane and dried *in vacuo* (0.0125 g, 0.005 mmol, 5%). The amount was too small for further analysis and characterization other than crystallographic.

Polymerization and Oligomerization Results. Reactions with ethylene were carried out in 200 mL high-pressure Büchi reactors containing a heating/cooling jacket. Every run was measured in triplicate and the data averaged. A preweighed amount of catalyst was dissolved in 100 mL of toluene under N_2 prior to loading the reaction vessel. Solutions were heated using a thermostatic bath and charged with ethylene, maintaining the pressure throughout the run. Polymerizations were quenched by releasing the pressure and addition of EtOH and HCl. The polymers obtained were isolated by filtration, sonicated with a solution of HCl, rinsed, and thoroughly dried prior to measuring the mass. The reaction mixtures of the oligomerization runs were cooled to 0 °C prior to releasing the overpressure and quenching with EtOH and HCl. Total oligomer yield was obtained by NMR upon

dx.doi.org/10.1021/om201181n | *Organometallics* XXXX, XXX, XXX−XXX

integration of the olefinic resonances versus the solvent and analyzed by GC-MS.

X-ray Crystallography. Suitable crystals were selected, mounted on a thin, glass fiber with paraffin oil, and cooled to the data collection temperature. Data were collected on a Bruker AXS SMART 1 k CCD diffractometer. Data collection was performed with three batch runs at phi = 0.00° (600 frames), at phi = 120.00° (600 frames), and at phi = 240.00° (600 frames). Initial unit-cell parameters were determined from 60 data frames collected at different sections of the Ewald sphere. Semiempirical absorption corrections based on equivalent reflections were applied. The systematic absences and unit-cell parameters were consistent for the reported space groups. The structures were solved by direct methods, completed with difference Fourier syntheses, and refined with full-matrix least-squares procedures based on F^2. All non-hydrogen atoms were refined with anisotropic displacement parameters. All hydrogen atoms were treated as idealized contributions. All scattering factors and anomalous dispersion factors are contained in the SHELXTL 6.12 program library. Relevant crystal data and bond distances and angles are given as SI.

Computational Methods. All calculations used the program Turbomole[25] in combination with the external Baker optimizer.[26] For the energy profile shown in Figures 3 and 4, all geometries were initially fully optimized at the b3-lyp[27]/TZVP[28] level. Vibrational analyses (analytical second derivatives) were carried out to check the nature of all stationary points (minima or transition states) and to calculate thermal corrections (enthalpy and entropy, gas phase, 273 K 1 bar). Since the calculations were not intended to model any specific experiment, no solvent corrections were applied, but entropies were scaled by a factor of 0.67 to represent the effect of reduced freedom in solution.[29] For all systems, improved single-point energies at the optimized geometries were then calculated at the b3-lyp/TZVPP[30] level. Final free energies were obtained by combining the b3-lyp/TZVPP electronic energy with the enthalpy and scaled entropy values obtained at the b3-lyp/TZVP level. Structures of model compounds $(Me_3P)Cr[\mu\text{-}MeNPMe_2]_3Cr$ (for **2**) and (η^4-butadiene)Cr(μ,η^4-butadienediyl)[μ-$MeNPMe_2$]$Mg(THF)_2$ and (η^4-butadiene)Cr(μ,η^4-butadien-diyl)[μ-$MeNPMe_2$]$Mg\ Cl_2^{2-}$ (for **3**) were only optimized at the b3-lyp[C]/SV(P)[31] level, and no higher-level single-point calculations were performed. Orbital plots were generated using Molden.[32]

■ ASSOCIATED CONTENT

Ⓢ Supporting Information

Crystallographic data (CIF) for the complexes reported in this paper and extensive listing of geometrical parameters. Magnetization plots at variable T and variable field for **2**. This material is available free of charge via the Internet at http://pubs.acs.org.

■ AUTHOR INFORMATION

Corresponding Author

*E-mail: sgambaro@uottawa.ca.

■ ACKNOWLEDGMENTS

This work was supported by NSERC, the University of Ottawa (S.G., M.M.), and the University of Manitoba (P.B.).

■ REFERENCES

(1) (a) Wass, D. *Dalton Trans.* **2007**, 816, and references therein. (b) Dixon, J. T.; Green, M. J.; Hess., F. M.; Morgan, D. H. *J. Organomet. Chem.* **2004**, *689*, 3641. (c) McGuinness, D. S. *Chem. Rev.* **2011**, *111*, 2321 , and references therein.

(2) (a) McDermott, J. X.; White, J. F.; Whitesides, G. M. *J. Am. Chem. Soc.* **1976**, *98*, 6521. (b) Manyik, R. M.; Walker, W. E.; Wilson, T. P. *J. Catal.* **1977**, *47*, 197. (c) McDaniel, M. P. *Adv. Catal.* **1985**, *33*, 47. (d) Briggs, J. R. *J. Chem. Soc., Chem. Commun.* **1989**, 674. (e) Meijboom, N.; Schaverien, C. J.; Orpen, A. G. *Organometallics* **1990**, *9*, 774. (f) Emrich, R.; Heinemann, O.; Jolly, P. W.; Kruger, C.; Verhovnik, G. P. J. *Organometallics* **1997**, *16*, 1511. (g) Köhn, R. D.; Haufe, M.; Kociok-Köhn, G.; Grimm, S.; Wasserscheid, P.; Keim, W. *Angew. Chem., Int. Ed.* **2000**, *39*, 4337. (h) Wang, M.; Shen, Y.; Qian, M.; Li, Rui, He, R. *J. Organomet. Chem.* **2000**, *599*, 143. (i) Carter, A.; Cohen, S. A.; Cooley, N. A.; Murphy, A.; Scutt, J.; Wass, D. F. *Chem. Commun.* **2002**, 858. (j) McGuinness, D. S.; Wasserscheid, P.; Keim, W.; Hu, C.; Englert, U.; Dixon, J. T.; Grove, C. *Chem. Commun.* **2003**, 334. (k) McGuinness, D. S.; Wasserscheid, P.; Keim, W.; Morgan, D. H.; Dixon, J. T.; Bollmann, A.; Maumela, H.; Hess, F. M.; Englert, U. *J. Am. Chem. Soc.* **2003**, *125*, 5272. (l) Morgan, D. H.; Schwikkard, H.; Dixon, J. T.; Nair, J. J.; Hunter, R. *Adv. Synth. Catal.* **2003**, *345*, 939. (m) Blok, A. N.; Budzelaar, P. H. M.; Gal, A. W. *Organometallics* **2003**, *22*, 2564. (n) Yu, Z.; Houk, K. N. *Angew. Chem., Int. Ed.* **2003**, *42*, 808. (o) Rensburg, W. J.; Grove, C.; Steynberg, J. P.; Stark, K. B.; Huyser, J. J.; Steynberg, P. J. *Organometallics* **2004**, *23*, 1207. (p) McGuinness, D. S.; Wasserscheid, P.; Morgan, D. H.; Dixon, J. T. *Organometallics* **2005**, *24*, 552. (q) Bluhm, M. E.; Walter, O.; Döring, M. *J. Organomet. Chem.* **2005**, *690*, 713. (r) Nenu, C. N.; Weckhuysen, B. M. *Chem. Commun.* **2005**, 1865. (s) Tomov, A. K.; Chirinos, J. J.; Jones, D. J.; Long, R. J.; Gibson, V. C. *J. Am. Chem. Soc.* **2005**, *127*, 10166. (t) Elowe, P. R.; McCann, C.; Pringle, P. G.; Spitzmesser, S. K.; Bercaw, J. E. *Organometallics* **2006**, *25*, 5255. (u) Agapie, T.; Labinger, J. A.; Brecaw, J. E. *J. Am. Chem. Soc.* **2007**, *129*, 14281. (v) McGuinness, D. S.; Suttil, J. A.; Gardiner, M. G.; Davies, N. W. *Organometallics* **2008**, *27*, 4238. (w) Zhang, J.; Braunstein, P.; Hor, T. S. A. *Organometallics* **2008**, *27*, 4277. (x) Zhang, J.; Li, A.; Hor, T. S. A. *Organometallics* **2009**, *28*, 2935. (y) Peitz, S.; Peulecke, N.; Aluri, B. R.; Hansen, S.; Müller, B. H.; Spannenberg, A.; Rosenthal, U.; Al-Hazmi, M. H.; Mosa, F. M.; Wöhl, A.; Müller, W. *Eur. J. Inorg. Chem.* **2010**, 1167. (z) Hey, T. W.; Wass, D. F. *Organometallics* **2010**, *29*, 3676. (aa) Köhn, R. D.; Haufe, M.; Mihan, S.; Lilge, D. *Chem. Commun.* **2000**, 1927.

(3) (a) Bollmann, A.; Blann, K.; Dixon, J. T.; Hess, F. M.; Killian, E.; Maumela, H.; McGuinness, D. S.; Morgan, D. H.; Neveling, A.; Otto, S.; Overett, M.; Slawin, A. M. Z.; Wasserscheid, P.; Kuhlmann, S. *J. Am. Chem. Soc.* **2004**, *126*, 14712. (b) Han, T.-K.; Ok, M. A.; Chae, S. S.; Kang, S. O. (SK Energy Corporation), WO 2008/088178, 2008. (c) Dulai, A.; McMullin, C. L.; Tenza, K.; Wass, D. F. *Organometallics* **2011**, *30*, 935. (d) Licciulli, S.; Thapa, I; Albahily, K.; Korobkov, I.; Gambarotta, S.; Duchateau, R.; Chevalier, R.; Schuhen, K. *Angew. Chem., Int. Ed.* **2010**, *49*, 9225.

(4) Groppo, E.; Lamberti, C.; Bordiga, S.; Spoto, G.; Zecchina, A. *J. Catal.* **2006**, *240*, 172.

(5) (a) Vidyaratne, I.; Nikiforov, G. B.; Gorelsky, S. I.; Gambarotta, S.; Duchateau, R. *Angew. Chem., Int. Ed.* **2009**, *48*, 6552. (b) Kurek, A.; Muelhaupt, R. *PMSE Prepr.* **2008**, *99*, 484. (c) Kurek, A.; Mark, S.; Enders, M.; Kristen, M. O.; Mülhaupt, R. *Macromol. Rapid Commun.* **2010**, *31*, 1359.

(6) (a) Lappin, G. R.; Sauer, J. D. In *Alpha Olefins Application Handbook*; Marcel Dekkers, Inc.: New York, 1989; Vol. 37, pp 1−3. (b) Vogt, D. Oligomerization of ethylene to higher linear R-olefins. In *Applied Homogeneous Catalysis with Organometallic Compounds*; Cornils, B., Herrmann, W. A., Eds.; Wiley-VCH: Weinheim, Germany, 2000; Chapter 2, pp 245−258. (c) Alpha Olefins (02/03-4), PERP Report, Mexant Chem Systems. (d) Lutz, E. F. *J. Chem. Educ.* **1986**, *63*, 202. (e) Weissermel, K.; Arpe, H.-J. In *Industrial Organic Chemistry*, 3rd ed.; John Wiley & Sons: New York, 1997; ISBN 3-527-28838-4. (f) Wittcoff, H.; Reuben, B. G.; Plotkin, J. S. In *Industrial Organic Chemicals*, 2nd ed.; Wiley-Interscience, 2004. (g) Kuhn, P.; Semeril, D.; Matt, D.; Chetcuti, M. J.; Lutz, P. *Dalton Trans.* **2007**, 515.

(7) (a) Bowen, L. E.; Haddow, M. F.; Orpen, A. G.; Wass, D. *Dalton Trans.* **2007**, 1160. (b) Rucklidge, A. J.; McGuinness, D. S.; Tooze, R. P.; Slawin, A. M. Z.; Pelletier, J. D. A; Hanton, M. J.; Webb, P. B. *Organometallics* **2007**, *26*, 2782. (c) Jabri, A.; Mason, C. B.; Sim, Y.; Gambarotta, S.; Burchell, T. J.; Duchateau, R. *Angew. Chem., Int. Ed.* **2008**, *47*, 9717. (d) Dulai, A.; de Bod, H.; Hanton, M. J.; Smith, D. M.; Downing, S.; Mansell, S. M.; Wass, D. F. *Organometallics* **2009**, *28*, 4613. (e) Licciulli, S.; Albahily, K.; Fomitcheva, V.; Korobkov, I.; Gambarotta, S.; Duchateau, R. *Angew. Chem., Int. Ed.* **2011**, *50*, 2346−2349.

(8) For a discussion see for example: Albahily, K.; Shaikh, Y.; Ahmed, Z.; Korobkov, I.; Gambarotta, S.; Duchateau, R. *Organometallics* **2011**, *30*, 4159 , and references therein.
(9) (a) McGuinness, D. S.; Gibson, V. C.; Steed, J. W. *Organometallics* **2004**, *23*, 6288. (b) Tenza, K.; Hanton, M. J.; Slawin, A. M. Z. *Organometallics* **2009**, *28*, 4852. (c) Albahily, K.; Licciulli, S.; Gambarotta, S.; Korobkov, I.; Chevalier, R.; Schuhen, K.; Duchateau, R. *Organometallics* **2011**, *30*, 3346. (d) Kirillov, E.; Roisnel, T.; Razavi, A.; Carpentier, J.-F. *Organometallics* **2009**, *28*, 2401. (e) Junges, F.; Kuhn, M. C. A.; dos Santos, A. H. D. P.; Rabello, C. R. K.; Thomas, C. M.; Carpentier, J.-F.; Casagrande, O. L. Jr. *Organometallics* **2007**, *26*, 4010. (f) Chen, Y.; Zuo, W.; Hao, P.; Zhang, S.; Gao, K.; Sun, W.-H. *J. Organomet. Chem.* **2008**, *693*, 750. (g) Gao, R.; Liang, T.; Wanga, F.; Sun, W.-H. *J. Organomet. Chem.* **2009**, *694*, 3701. (h) Small, B. L.; Rios, R.; Fernandez, E. R.; Gerlach, D. L.; Halfen, J. A.; Carney, M. J. *Organometallics* **2010**, *29*, 6723−6731. (i) Albahily, K.; Ahmed, Z.; Gambarotta, S.; Koç, E.; Duchateau, R.; Korobkov, I. *Organometallics* **2011**, *30*, 6022−6027.
(10) See for example: (a) Temple, C.; Jabri, A.; Crewdson, P.; Gambarotta, S.; Korobkov, I.; Duchateau, R. *Angew. Chem., Int. Ed.* **2006**, *45*, 7050. (b) Jabri, A.; Crewdson, P.; Gambarotta, S.; Korobkov, I.; Duchateau, R. *Organometallics* **2006**, *25*, 715. (c) Jabri, A.; Temple, C.; Crewdson, P.; Gambarotta, S.; Korobkov, I.; Duchateau, R. *J. Am. Chem. Soc.* **2006**, *128*, 9238.
(11) (a) Albahily, K.; Shaikh, Y.; Sebastiao, E.; Gambarotta, S.; Korobkov, I.; Gorelsky, S. *J. Am. Chem. Soc.* **2011**, *133*, 6388. (b) Albahily., K.; Fomitcheva, V.; Gambarotta, S.; Korobkov, I.; Murugesu, M.; Gorelski, S. *J. Am. Chem. Soc.* **2011**, *133*, 638.
(12) (a) McGuinness, D. S.; Wasserscheid, P.; Morgan, D. H.; Dixon, J. T. *Organometallics* **2005**, *24*, 552. (b) McGuinness, D. S.; Brown, D. B.; Tooze, R. P.; Hess, F. M.; Dixon, J. T.; Slawin, A. M. Z. *Organometallics* **2006**, *25*, 3605.
(13) (a) Peitz, S.; Peulecke, N.; Aluri, B. P.; Hansen, S.; Muller, B. H.; Spannenberg, A.; Rosenthal, U.; Al-Hazmi, M. H.; Mosa, F. M.; Wohl, A.; Muller, W. *Eur. J. Inorg. Chem.* **2010**, 1167. (b) Wohl, A.; Muller, W.; Peitz, S.; Peulecke, N.; Aluri, B. P.; Muller, B. H.; Heller, D.; Rosenthal, U.; Al-Hazmi, M. H.; Mosa, F. M. *Chem.—Eur. J.* **2010**, *16*, 7833. (c) Peitz, S.; Peulecke, N.; Aluri, B. P.; Muller, B. H.; Spannenberg, A.; Rosenthal, U.; Al-Hazmi, M. H.; Mosa, F. M.; Wohl, A.; Muller, W. *Organometallics* **2010**, *29*, 5263. (d) Aluri, B. R.; Peulecke, N.; Peitz, S.; Spannenberg, A.; Müller, B. H.; Schulz, S.; Heller, D.; Al-Hazmi, M. H.; Mosa, F. M.; Wöhl, A.; Müller, W.; Rosenthal, U. *Dalton Trans.* **2010**, 7911. (e) Peulecke, N.; Muller, W.; Peitz, S.; Aluri, B. P.; Rosenthal, U.; Wohl, A.; Muller, B. H.; Al-Hazmi, M. H.; Mosa, F. M. *Chem. Catal. Chem* **2010**, *2*, 1079.
(14) Blann, K.; Bollmann, A.; Dixon, J. T.; Neveling, A.; Morgan, D. H.; Maumela, H.; Killian, E.; Hess, F. M.; Otto, S.; Pepler, L.; Mahomed, H. A.; Overett, M. J. (Sasol Technology LTD) WO 04/056479, 2004.
(15) Dulai, A.; McMullin, C. L.; Tenza, K.; Wass., D. F. *Organometallics* **2011**, *30*, 935.
(16) Albahily., K.; Fomitcheva, V.; Shaikh, Y.; Sebastiao, E.; Gambarotta, S.; Korobkov, I.; Duchateau, R. *Organometallics* **2011**, *30*, 4201.
(17) (a) Albahily, K.; Al-Baldawi, D.; Gambarotta, S.; Duchateau, R.; Koç, E.; Burchell., T. J. *Organometallics* **2008**, *27*, 22. (b) Albahily, K.; Al-Baldawi, D.; Gambarotta, S.; Duchateau, R.; Koç, E.; Burchell, T. J. *Organometallics* **2008**, *27*, 5943. (c) Albahily, K.; Koç, E.; Al-Baldawi, D.; Savard, D.; Gambarotta, S.; Burchell, T. J.; Duchateau, R. *Angew. Chem., Int. Ed.* **2008**, *47*, 5816.
(18) Thapa, I.; Gambarotta, S.; Duchateau, R.; Kulangara, S. V.; Chevalier, R. *Organometallics* **2010**, *29*, 4080.
(19) Peitz, S.; Aluri, B. R.; Peulecke, N.; Muller, B. H.; Wohl, A.; Muller, W.; Al-Hazmi, M. H.; Mosa, F. M.; Rosenthal, U. *Chem.—Eur. J.* **2010**, *16*, 7670.
(20) Reardon, D.; Kovacs, I.; Ruppa, K. B. P.; Feghali, K.; Gambarotta, S.; Petersen, J. *Chem.—Eur. J.* **1997**, *3*, 1482.
(21) The unrestricted calculation result has Cr(I) with 1 α- and 4 β-electrons, and Cr(II) with 4 α-electrons. This is likely an artifact of the use of a single determinant instead of a well-defined spin state.
(22) Horvath, S.; Gorelski, S.; Gambarotta, S; Korobkov, I. *Angew. Chem., Int. Ed.* **2008**, *47*, 3723.
(23) Budzelaar, P. H. M. *Can. J. Chem.* **2009**, *87*, 832.
(24) Budzelaar, P. H. M.; Talarico, G. *Organometallics* **2008**, *27*, 4098.
(25) (a) Ahlrichs, R.; Bär, M.; Baron, H.-P.; Bauernschmitt, R.; Böcker, S.; Ehrig, M.Eichkorn, K.; Elliott, S.; Furche, F.; Haase, F.; Häser, M.; Hättig, C.; Horn, H.; Huber, C.; Huniar, U.; Kattannek, M.; Köhn, A.; Kölmel, C.; Kollwitz, M.; May, K.; Ochsenfeld, C.; Ohm, H.; Schäfer, A.; Schneider, U.; Treutler, O.; Tsereteli, K.; Unterreiner, B.; Von Arnim, M.; Weigend, F.; Weis, P.; Weiss, H. *Turbomole*, 5 ed.; Theoretical Chemistry Group, University of Karlsruhe, 2002. (b) Treutler, O.; Ahlrichs, R. *J. Chem. Phys.* **1995**, *102*, 346.
(26) (a) Baker, J. *J. Comput. Chem.* **1986**, *7*, 385. (b) Baker, J. *PQS*, 2.4 ed.; Parallel Quantum Solutions: Fayetteville, AR, 2001.
(27) (a) Becke, A. D. *J. Chem. Phys.* **1993**, *98*, 5648. (b) Becke, A. D. *J. Chem. Phys.* **1993**, *98*, 1372. (c) Lee, C. T.; Yang, W. T.; Parr, R. G. *Phys. Rev. B* **1988**, *37*, 785.
(28) Schafer, A.; Huber, C.; Ahlrichs, R. *J. Chem. Phys.* **1994**, *100*, 5829.
(29) (a) Raucoules, R.; de Bruin, T.; Raybaud, P.; Adamo, C. *Organometallics* **2009**, *28*, 5358. (b) Tobisch, S.; Ziegler, T. *J. Am. Chem. Soc.* **2004**, *126*, 9059.
(30) Weigend, F.; Furche, F.; Ahlrichs, R. *J. Chem. Phys.* **2003**, *119*, 12753.
(31) Schafer, A.; Horn, H.; Ahlrichs, R. *J. Chem. Phys.* **1992**, *97*, 2571.
(32) Schaftenaar, G.; Noordik, J. H. *J. Comput.-Aided Mol. Des.* **2000**, *14*, 123.